A Multi-Resolution Scheme for Analysis of Brain Connectivity Networks

Vikas Singh

Biostatistics, Computer Sciences

THE UNIVERSITY of WISCONSIN MADISON

Mathematical and Statistical Challenges in Neuroimaging Data Analysis
October 2015

Joint work with Nagesh Adluru, Emily Balczewski, Barb Bendlin, Moo Chung, SeongJae Hwang, Sterling Johnson, WonHwa Kim and Ozioma Okonkwo

Motivation

Group analysis of image derived representations

Motivation

Group analysis of image derived representations

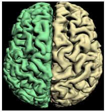

...

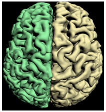

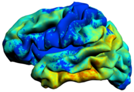

Motivation

Group analysis of image derived representations

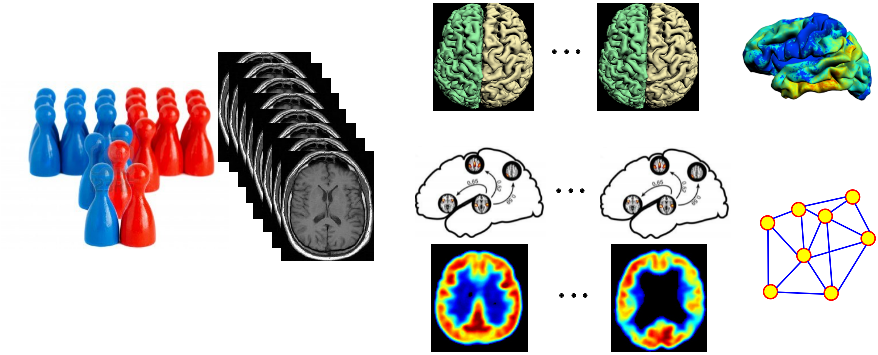

Workflow

- Lots of QC and corrections
- Figure out how to warp one image to another
- Perform atom-wise statistical analysis after a laundry list of pre-processing

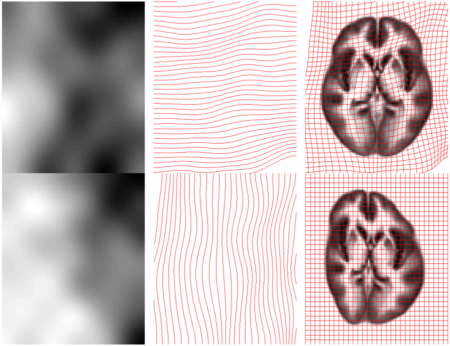

Workflow

- Lots of QC and corrections
- Figure out how to warp one image to another
- Perform atom-wise statistical analysis after a laundry list of pre-processing

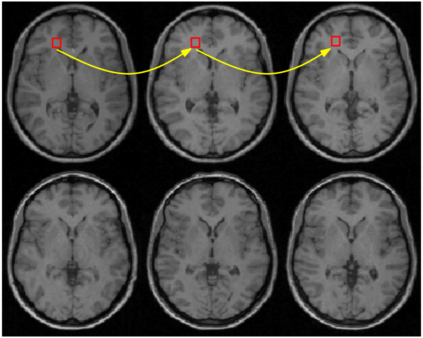

Workflow

- Lots of QC and corrections
- Figure out how to warp one image to another
- Perform atom-wise statistical analysis after a laundry list of pre-processing

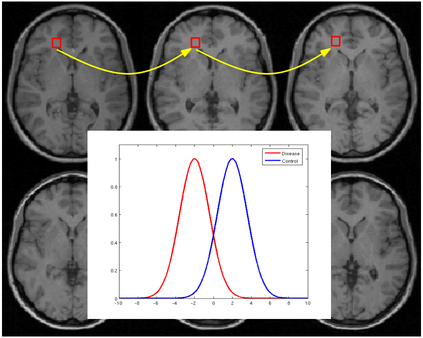

Finally obtain heat maps of discriminative voxels (after p-value corrections)

Figure 7a

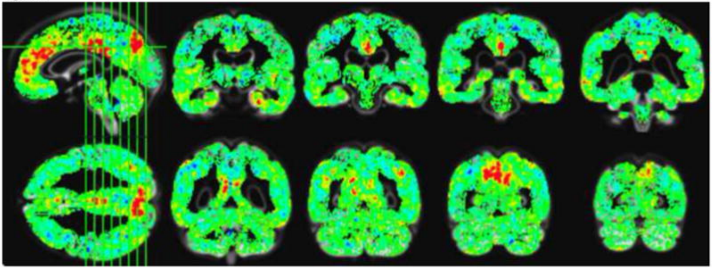

Figure 7b

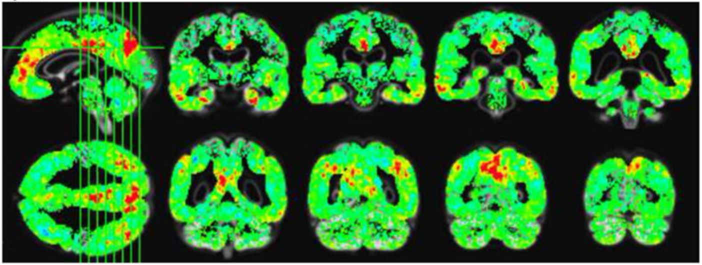

Voxel wise analysis on the Image grid

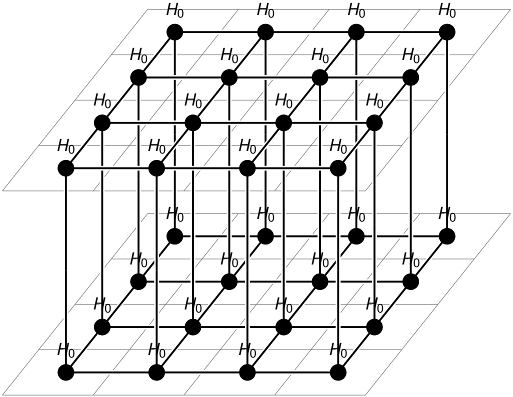

Voxel wise analysis on the Image grid

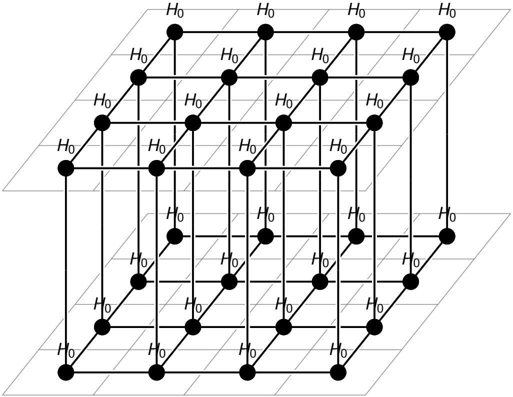

The multiple testing problem is significant especially when testing at a million **(independent?)** voxels

Type 1 and Type 2 Errors in Neuroimaging

	H_0 is true voxel not discriminative	H_0 is false voxel is discriminative
Reject H_0	Type 1 Error (false positive)	Correct
$\neg$**Reject** H_0	Correct	Type 2 Error (false negative)

To be safe on Type 1 errors, a super conservative strategy may lead to many false negatives

Analysis of cortical meshes

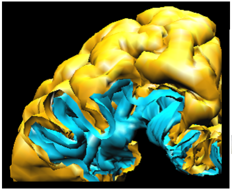

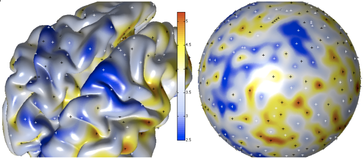

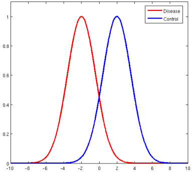

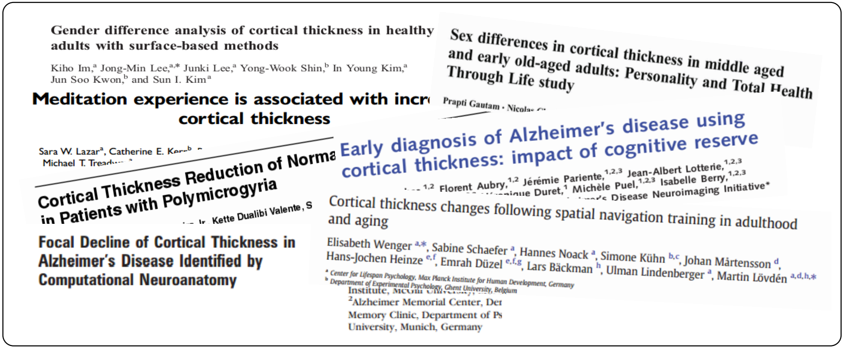

Gender difference analysis of cortical thickness in healthy adults with surface-based methods

Kiho Im,[a] Jong-Min Lee,[a,*] Junki Lee,[a] Yong-Wook Shin,[b] In Young Kim,[a] Jun Soo Kwon,[b] and Sun I. Kim[a]

Sex differences in cortical thickness in middle aged and early old-aged adults: Personality and Total Health Through Life study

Meditation experience is associated with incr… cortical thickness

Sara W. Lazar[a], Catherine E. Kerr[b] …

Early diagnosis of Alzheimer's disease using cortical thickness: impact of cognitive reserve

Florent Aubry,[1,2] Jérémie Pariente,[1,2,3] Jean-Albert Lotterie,[1,2,3] Michèle Puel,[1,2,3] Isabelle Berry,[1,2,3]

Cortical Thickness Reduction of Norma… in Patients with Polymicrogyria

Kette Dualibi Valente, …

Cortical thickness changes following spatial navigation training in adulthood and aging

Elisabeth Wenger [a,*], Sabine Schaefer [a], Hannes Noack [a], Simone Kühn [b,c], Johan Mårtensson [d], Hans-Jochen Heinze [e,f], Emrah Düzel [e,f,g], Lars Bäckman [h], Ulman Lindenberger [a], Martin Lövdén [a,d,h,*]

[a] Center for Lifespan Psychology, Max Planck Institute for Human Development, Germany
[b] Department of Experimental Psychology, Ghent University, Belgium

Focal Decline of Cortical Thickness in Alzheimer's Disease Identified by Computational Neuroanatomy

[2]Alzheimer Memorial Center, De…
Memory Clinic, Department of Ps…
University, Munich, Germany

Analysis of connectivity networks

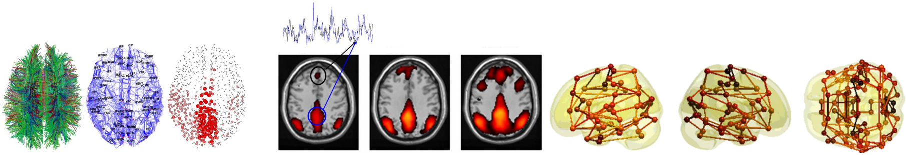

Functional connectivity tracks clinical deterioration in Alzheimer's disease

Jessica S. Damoiseaux[a,*], Katherine E. Prater[b], Bruce L. Miller[c], Michael ...

Resting state functional MRI in Alzheimer's Disease

Prashanthi Vemuri[*1], David T Jones[2] and Clifford R Jack Jr.[1]

Characterizing functional connectivity differences in aging adults using machine learning on resting state fMRI data

Neurobiology of Disease

APOE4 Allele Disrupts Resting State fMRI Connectivity in the Absence of Amyloid Plaques or Decreased CSF Aβ42

Adult age differences in functional connectivity during executive control

David J. Madden[a,b,c,*], Matthew C. Costello[a], Nancy A. Dennis[a,c], Simon W. Davis[c], Anne M. Shepler
Julia Spaniol[a], Barbara Bucur[a], Roberto Cabeza[c]

...RAL CORRELATES MEDIATING AGE DIFFERENCES IN ...ODIC MEMORIES: EVIDENCE FROM BOLD CONTRASTS AND CONNECTIVITY ANALYSES

Dynamic causal modelling of effective connectivity from fMRI: Are results reproducible and sensitive to Parkinson's disease and its treatment?

J.B. Rowe[a,b,c,*], L.E. Hughes[a,b], R.A. Barker[a,d], and A.M. Owen[b]

Effects of aging on functional connectivity of the amygdala during negative evaluation: A network analysis of fMRI data

Peggy St. Jacques[a, b], Florin Dolcos[a, c, 1], Roberto Cabeza[a, b]

DTI Tractography

White matter orientational information from DTI

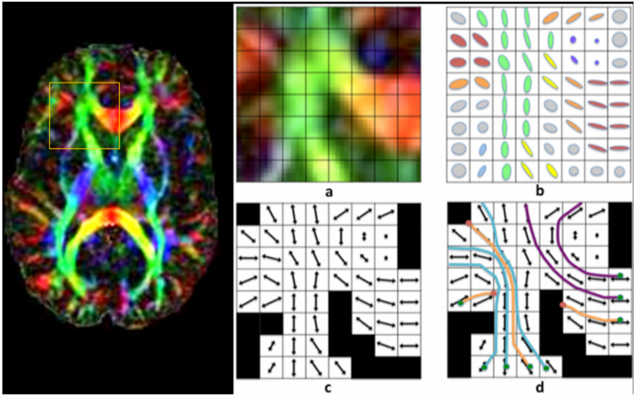

DTI Tractography

Streamline fiber tracking from orientation field

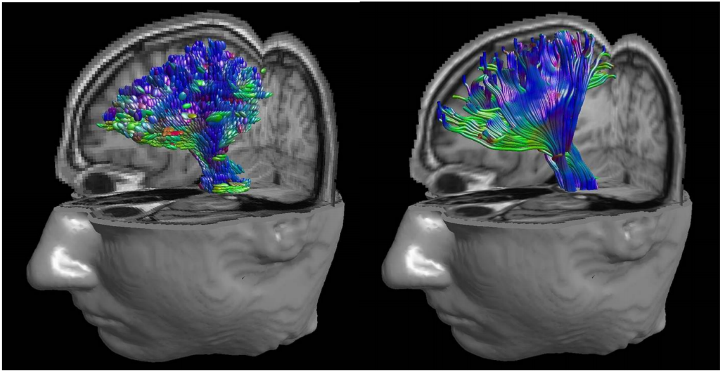

DTI Tractography

Brain atlas and connectivity matrix

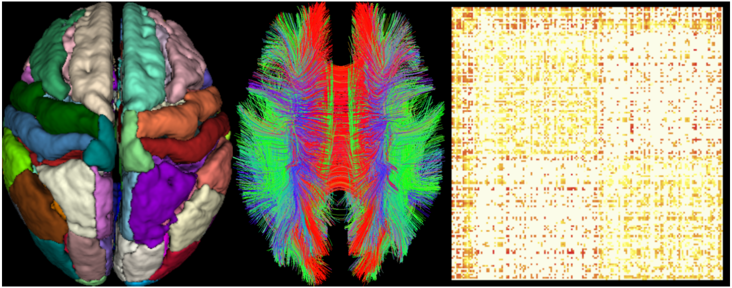

Analysis questions

Challenges

- Statistical analysis on connectivity matrix involves $\mathcal{O}(n^2)$ terms
- Sample sizes are small in Neuroimaging studies: large p, small n
- The "connectivity" between different "nodes" of the graph is arbitrary

Analysis questions

Challenges

- Statistical analysis on connectivity matrix involves $\mathcal{O}(n^2)$ terms
- Sample sizes are small in Neuroimaging studies: large p, small n
- The "connectivity" between different "nodes" of the graph is arbitrary

Need for methods which are sensitive to small signal differences

- Multi-resolution analysis of shapes and connectivity networks

Analysis questions

Challenges

- Statistical analysis on connectivity matrix involves $\mathcal{O}(n^2)$ terms
- Sample sizes are small in Neuroimaging studies: large p, small n
- The "connectivity" between different "nodes" of the graph is arbitrary

Analysis questions

Challenges

- Statistical analysis on connectivity matrix involves $\mathcal{O}(n^2)$ terms
- Sample sizes are small in Neuroimaging studies: large p, small n
- The “connectivity” between different “nodes” of the graph is arbitrary

Analysis questions

Challenges

- Statistical analysis on connectivity matrix involves $\mathcal{O}(n^2)$ terms
- Sample sizes are small in Neuroimaging studies: large p, small n
- The "connectivity" between different "nodes" of the graph is arbitrary

- Identifying "differences" is related to finding "similarity".
- Comparison of signals in multiple resolutions
- E.g., SIFT feature
- An end-to-end statistical explanation as well (with some disclaimer)

Analysis questions

Challenges

- Statistical analysis on connectivity matrix involves $\mathcal{O}(n^2)$ terms
- Sample sizes are small in Neuroimaging studies: large p, small n
- The "connectivity" between different "nodes" of the graph is arbitrary

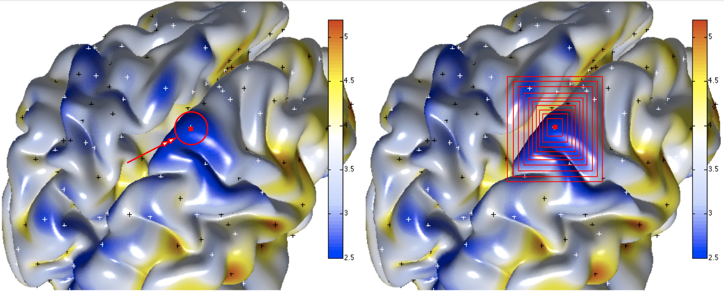

Analysis questions

Challenges

- Statistical analysis on connectivity matrix involves $\mathcal{O}(n^2)$ terms
- Sample sizes are small in Neuroimaging studies: large p, small n
- The "connectivity" between different "nodes" of the graph is arbitrary

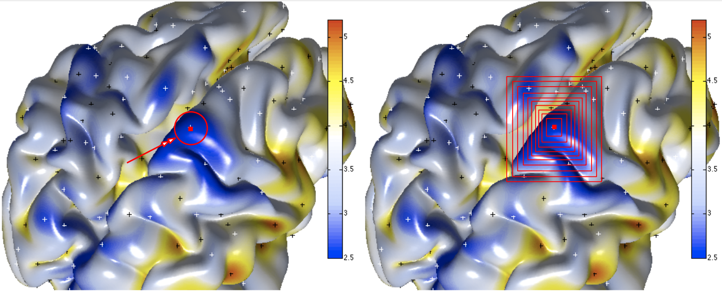

Wavelets?

Fourier Transform

- Superposition of sinusodial functions $e^{i\omega t}$ in different frequencies
- Fourier Transform of $f(x)$:
  (From native space to the frequency space)

$$\boxed{\hat{f}(\omega) = \int f(x)\mathrm{e}^{-j\omega x}\mathrm{d}x}$$

Fourier Transform

- Superposition of sinusodial functions $e^{i\omega t}$ in different frequencies
- Fourier Transform of $f(x)$:
  (From native space to the frequency space)

$$\boxed{\hat{f}(\omega) = \int f(x) \mathrm{e}^{-j\omega x} \mathrm{d}x}$$

- Inverse Fourier Transform:
  (Reconstruct my signal)

$$\boxed{f(x) = \frac{1}{2\pi} \int \hat{f}(\omega) \mathrm{e}^{j\omega x} \mathrm{d}\omega}$$

Weather in Madison affects forecast in Banff

- Ringing Artifact (e.g., Gibbs phenomenon)
  (caused by infinite support of Fourier bases)

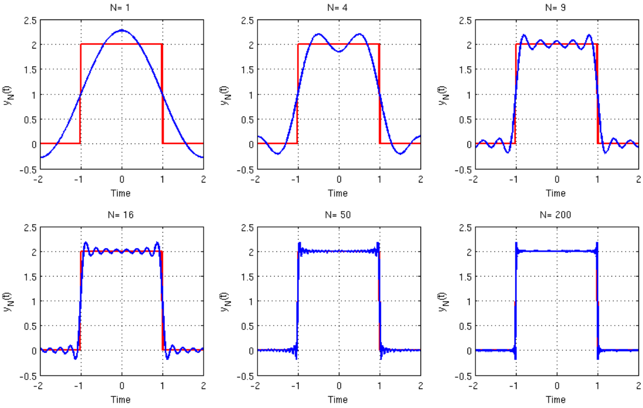

Figure: Ringing artifact using Fourier bases.

Wavelet Transform

Wavelet bases

Unlike Fourier bases, Wavelets are **localized in both time and frequency**

Wavelet Transform

Wavelet bases

Unlike Fourier bases, Wavelets are **localized in both time and frequency**

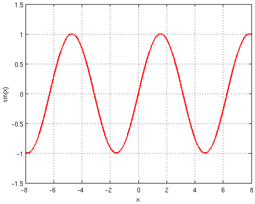

Sine

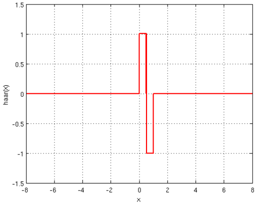

Haar Wavelet

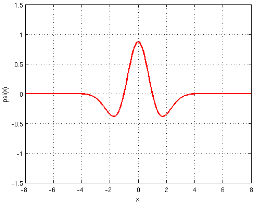

Mexican hat wavelet

Wavelet Transform

- Mother wavelet ψ: function of dilation s and translation a

$$\boxed{\psi_{s,a}(x) = \frac{1}{s}\psi\left(\frac{x-a}{s}\right)}$$

Wavelet Transform

- Mother wavelet ψ: function of dilation s and translation a

$$\boxed{\psi_{s,a}(x) = \frac{1}{s}\psi\left(\frac{x-a}{s}\right)}$$

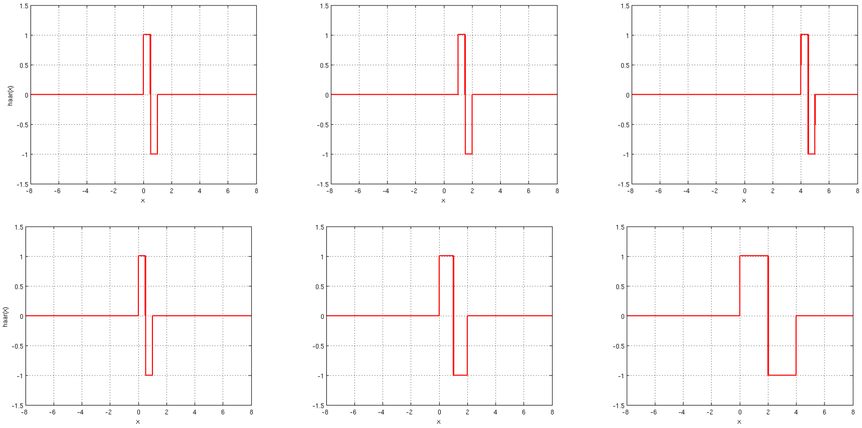

Wavelet Transform

Fourier

$$\hat{f}(\omega) = \int f(x)\mathrm{e}^{-j\omega x}\mathrm{d}x$$

Wavelets

$$W_f(s, a) = \frac{1}{s}\int f(x)\psi^*(\frac{x-a}{s})\mathrm{d}x$$

Wavelet Transform

Fourier

$$\hat{f}(\omega) = \underbrace{\int f(x) \mathrm{e}^{-j\omega x} \mathrm{d}x}_{\langle f, basis \rangle}$$

Wavelets

$$W_f(s, a) = \frac{1}{s} \underbrace{\int f(x) \psi^*(\frac{x-a}{s}) \mathrm{d}x}_{\langle f, basis \rangle}$$

Wavelet Transform

Fourier

$$\hat{f}(\omega) = \underbrace{\int f(x) \mathrm{e}^{-j\omega x} \mathrm{d}x}_{\langle f, basis \rangle}$$

Wavelets

$$W_f(s, a) = \frac{1}{s} \underbrace{\int f(x) \psi^*(\frac{x-a}{s}) \mathrm{d}x}_{\langle f, basis \rangle}$$

Inverse Fourier

$$f(x) = \frac{1}{2\pi} \int \hat{f}(\omega) \mathrm{e}^{j\omega x} \mathrm{d}\omega$$

Inverse Wavelets

$$f(x) = \frac{1}{C_\psi} \iint W_f(s, a) \psi_{s,a}(x) \mathrm{d}a \, \mathrm{d}s$$

Wavelet Transform

Fourier

$$\hat{f}(\omega) = \underbrace{\int f(x)\mathrm{e}^{-j\omega x}\mathrm{d}x}_{\langle f, basis\rangle}$$

Wavelets

$$W_f(s,a) = \frac{1}{s}\underbrace{\int f(x)\psi^*(\frac{x-a}{s})\mathrm{d}x}_{\langle f, basis\rangle}$$

Inverse Fourier

$$f(x) = \frac{1}{2\pi}\int \hat{f}(\omega)\mathrm{e}^{j\omega x}\mathrm{d}\omega$$

Inverse Wavelets

$$f(x) = \frac{1}{C_\psi}\iint W_f(s,a)\psi_{s,a}(x)\mathrm{d}a\,\mathrm{d}s$$

Admissibility Condition with $C_\psi = \int \frac{|\Psi(j\omega)|^2}{|\omega|}\mathrm{d}\omega < \infty$

To define C_ψ, $\Psi(j\omega) = \int \psi(t)e^{-j\omega t}\mathrm{d}t$

Wavelet in the Frequency Domain

- ψ (blue) in the frequency domain: band-pass filters
- ϕ (red) in the frequency domain: low-pass filter

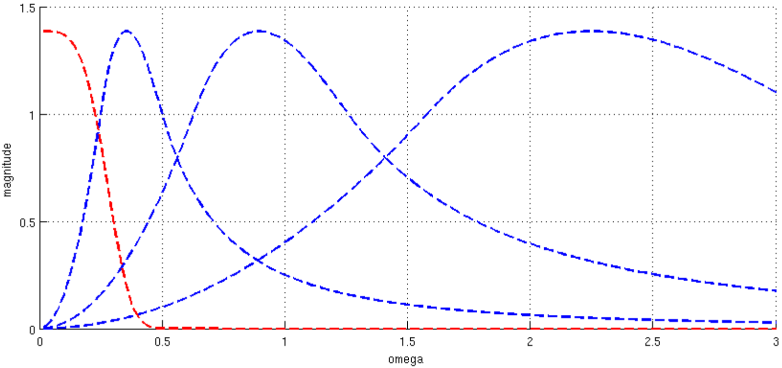

Figure: A scaling function (red) and band-pass filters (blue) in the frequency domain.

Classical Wavelet example

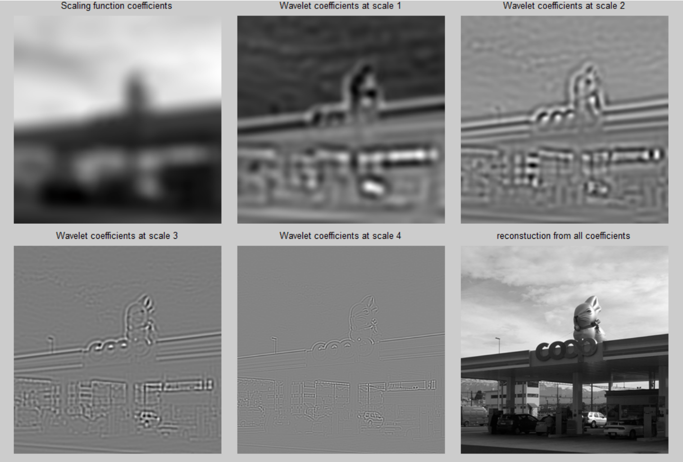

Figure: Example of multi-resolutional characterization (from SGWT toolbox)

Wavelet Transform on Graphs

- Wavelets in Euclidean Space

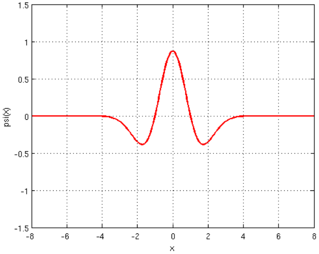

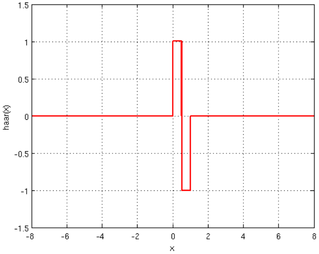

Wavelet Transform on Graphs

- Wavelets in Euclidean Space

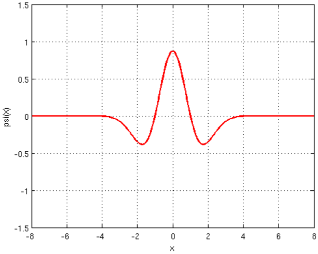

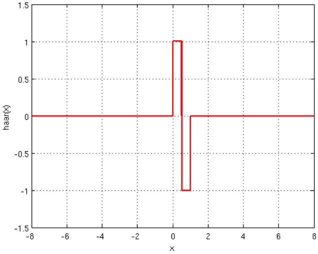

- Wavelets on Graphs
  (Scale? Translation?)

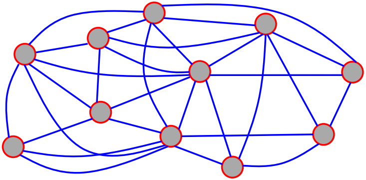

Wavelet Transform on Graphs

Key Idea

- Native domain: $G = \{V, E, \omega\}$
- First step: define analogue of Fourier transform on graphs (Maggioni, 2006), (Hammond 2012)
- Construct orthonormal bases defined on structure of G
- Construction of filters in the frequency domain to get band pass effect

Wavelet Transform on Graphs

Key Idea

- Native domain: $G = \{V, E, \omega\}$
- First step: define analogue of Fourier transform on graphs (Maggioni, 2006), (Hammond 2012)
- Construct orthonormal bases defined on structure of G
- Construction of filters in the frequency domain to get band pass effect

Ingredients

- Adjacency A: square matrix, $a_{m,n}$ for connectivity information
- Degree Matrix: D: Diagonals are the sum of weights
- Graph Laplacian: $L = D - A$
- Orthonormal bases χ_l and eigenvalues λ_l, $l \in \{0, \cdots, N-1\}$ of L

Wavelet Transform on Graphs

Key Idea

- Native domain: $G = \{V, E, \omega\}$
- First step: define analogue of Fourier transform on graphs (Maggioni, 2006), (Hammond 2012)
- Construct orthonormal bases defined on structure of G
- Construction of filters in the frequency domain to get band pass effect

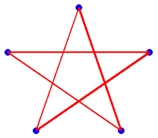

Star shaped graph

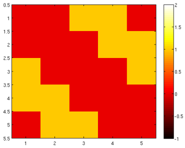

Adjacency

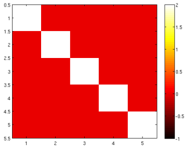

Degree

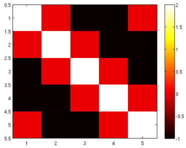

Laplacian

Wavelet Transform on Graphs

Fourier

$$\hat{f}(\omega) = \langle f, e^{j\omega x} \rangle = \int f(x) \mathrm{e}^{-j\omega x} \mathrm{d}x$$

Graph Fourier

$$\hat{f}(l) = \langle f, \chi_l \rangle = \sum_{n=1}^{N} f(n) \chi_l^*(n)$$

For graph Fourier transform, the orthonormal bases come from spectral graph theory: from a self-adjoint operator (the graph Laplacian)

Wavelet Transform on Graphs

Fourier

$$\hat{f}(\omega) = \langle f, e^{j\omega x} \rangle = \int f(x) \mathrm{e}^{-j\omega x} \mathrm{d}x$$

Graph Fourier

$$\hat{f}(l) = \langle f, \chi_l \rangle = \sum_{n=1}^{N} f(n) \chi_l^*(n)$$

For graph Fourier transform, the orthonormal bases come from spectral graph theory: from a self-adjoint operator (the graph Laplacian)

Inverse Fourier

$$f(x) = \frac{1}{2\pi} \int \hat{f}(\omega) \mathrm{e}^{j\omega x} \mathrm{d}\omega$$

Inverse Graph Fourier

$$f(n) = \sum_{l=0}^{N-1} \hat{f}(l) \chi_l(n)$$

Wavelet Transform on Graphs

Fourier

$$\hat{f}(\omega) = \langle f, e^{j\omega x} \rangle = \int f(x) \mathrm{e}^{-j\omega x} \mathrm{d}x$$

Graph Fourier

$$\hat{f}(l) = \langle f, \chi_l \rangle = \sum_{n=1}^{N} f(n) \chi_l^*(n)$$

For graph Fourier transform, the orthonormal bases come from spectral graph theory: from a self-adjoint operator (the graph Laplacian)

Inverse Fourier

$$f(x) = \frac{1}{2\pi} \int \hat{f}(\omega) \mathrm{e}^{j\omega x} \mathrm{d}\omega$$

Inverse Graph Fourier

$$f(n) = \sum_{l=0}^{N-1} \hat{f}(l) \chi_l(n)$$

- Construct original signal using graph Fourier bases and coefficients $\hat{f}$
- $L \succeq 0$, so χ and χ^* are the same.

Wavelet Transform on Graphs

Wavelet function on node m, localized on node n

$$\boxed{\psi_{s,n}(m) = \sum_{l=0}^{N-1} g(s\lambda_l)\chi_l^*(n)\chi_l(m)}$$

Choose a kernel function g (band-pass filter)

Wavelet Transform on Graphs

Wavelet function on node m, localized on node n

$$\boxed{\psi_{s,n}(m) = \sum_{l=0}^{N-1} g(s\lambda_l)\chi_l^*(n)\chi_l(m)}$$

Choose a kernel function g (band-pass filter)

Spectral Graph Wavelet Transform on $f(n)$ on node n

$$\boxed{W_f(s,n) = \sum_{l=0}^{N-1} g(s\lambda_l)\hat{f}(l)\chi_l(n)}$$

An Example of Wavelet Functions on Graphs

Example of wavelets on graphs (mesh surface)

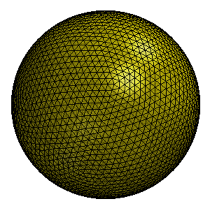

Mesh surface (sphere)

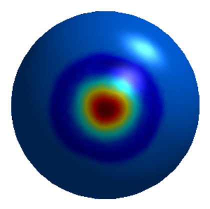

Mexican hat wavelet at scale 1

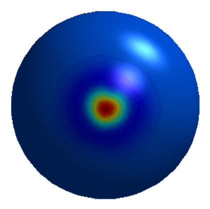

Mexican hat wavelet at scale 2

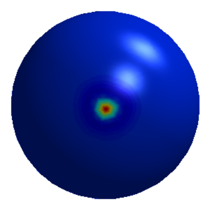

Mexican hat wavelet at scale 3

An Example of Wavelet Transform on Graphs

Forward and inverse wavelet transform of $f(n)$ (on a brain mesh)

$$\boxed{W_f(s,n) = \langle f, \psi_{s,n} \rangle = \sum_{l=0}^{N-1} g(s\lambda_l)\hat{f}(l)\chi_l(n)}$$

$$\boxed{f(n) = \frac{1}{C_g} \sum_{n=1}^{N} \int_0^{\infty} W_f(s,n)\psi_{s,n}(m)\frac{ds}{s}}$$

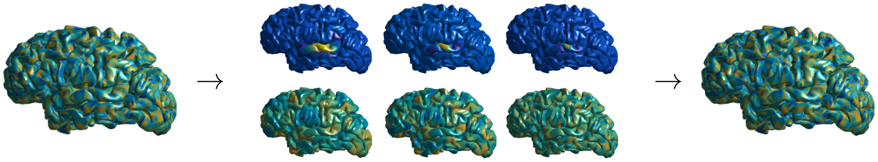

Figure: Forward and Inverse wavelet transform.

Application 1: Cortical Thickness Discrimination

- Group analysis: Identify regions showing differences between disparate groups
  - Alzheimer's disease versus Healthy controls
- Statistical Parametric Mapping
  - Hypothesis test at vertex level
  - Multiple comparison correction (Bonferroni, etc.)
  - Check which regions survive

Application 1: Cortical Thickness Discrimination

- Group analysis: Identify regions showing differences between disparate groups
  - Alzheimer's disease versus Healthy controls
- Statistical Parametric Mapping
  - Hypothesis test at vertex level
  - Multiple comparison correction (Bonferroni, etc.)
  - Check which regions survive

Domain: Brain surface mesh;
Signal: Cortical thickness (distance between inner/outer cortical surfaces)

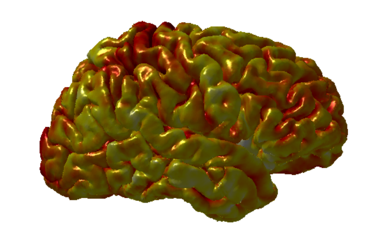

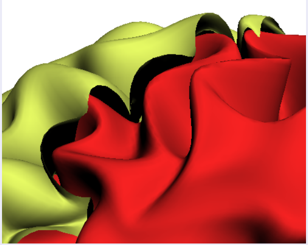

Application 1: Cortical Thickness Discrimination

- Wavelet multi-scale descriptor (WMD):
  - A set of wavelet coefficients at each vertex n for each scale s

$$\boxed{\mathrm{WMD}_f(n) = \{W_f(s, n) | s \in S\}} \tag{1}$$

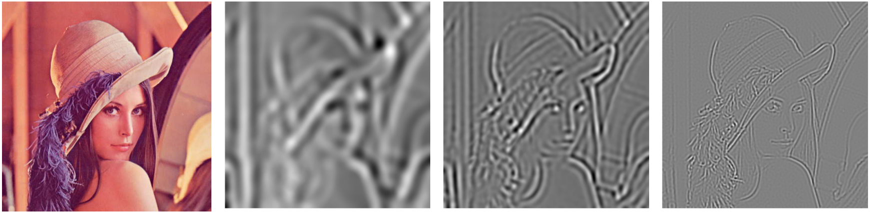

WMD on Lenna at scale 0, 1, 2.

Application 1: Cortical Thickness Discrimination

- Wavelet multi-scale descriptor (WMD):
  - A set of wavelet coefficients at each vertex *n* for each scale *s*

$$\boxed{\mathrm{WMD}_f(n) = \{W_f(s, n) | s \in S\}} \qquad (1)$$

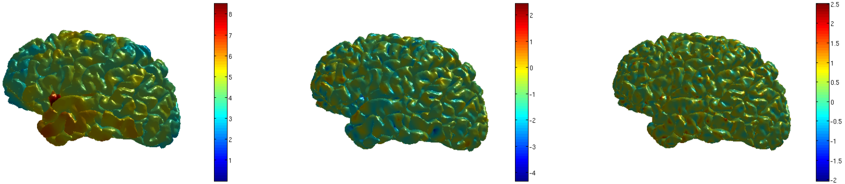

WMD on cortical thickness at scale 0, 1, 2.

Application 1: Cortical Thickness Discrimination (ADNI)

- Group analysis: Alzheimer's disease (AD) subjects versus healthy controls

Table: ADNI data details

ADNI data				
Category	AD (mean)	AD (s.d.)	Ctrl (mean)	Ctrl (s.d.)
# of Subjects	160	-	196	-
Age	75.53	7.41	76.09	5.13
Gender (M/F)	86 / 74	-	101 / 95	-
MMSE at Baseline	21.83	5.98	28.87	3.09
Years of Education	13.81	4.61	15.87	3.23

Application 1: Cortical Thickness Discrimination (ADNI)

- p-values from Hotelling's T^2. Then, multiple comparison correction

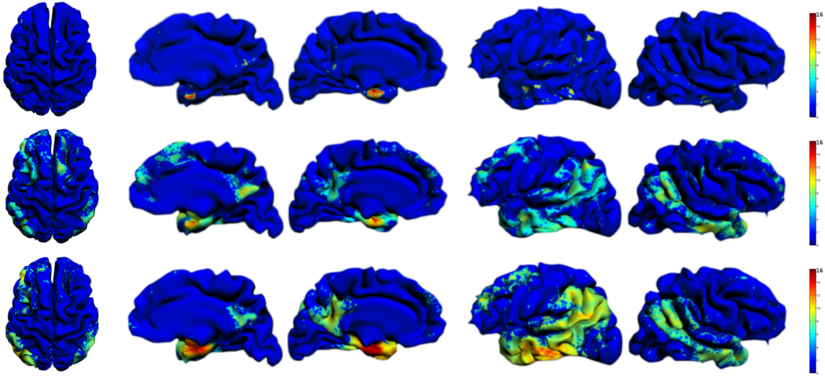

Figure: p-values (in $-\log_{10}$ scale) after FDR correction at $q = 10^{-5}$. Row 1: Cortical thickness, Row 2: SPHARM, Row 3: WMD

Application 1: Cortical Thickness Discrimination (ADNI)

- p-values and False discovery rate (FDR)
- Group difference: the vertices below the FDR threshold

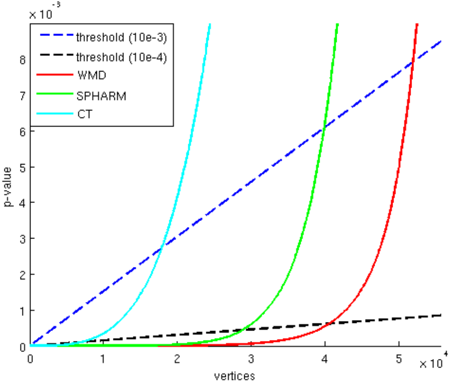

Figure: Sorted p-values from group analysis on cortical thickness (cyan), SPHARM (green), and WMD (red), and the FDR thresholds are represented by dotted lines.

Application 1: Cortical Thickness Discrimination (ADNI)

- Effect of changes of q in FDR

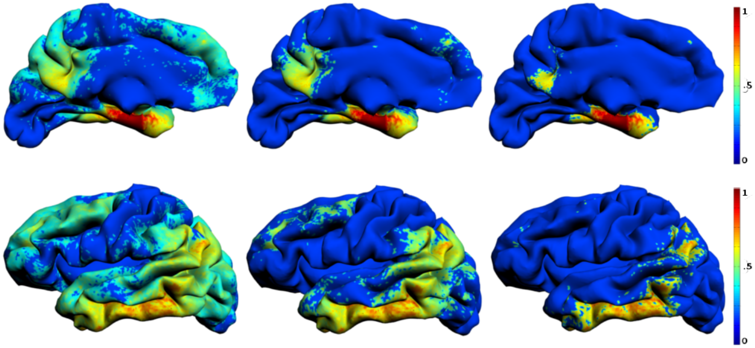

Figure: p-values (in $-\log_{10}$ scale and normalized) showing the effect of FDR correction on a left hemisphere using WMD with FDR $q = 10^{-3}$ (left column), $q = 10^{-5}$ (middle column) and $q = 10^{-7}$ (right column) respectively.

Application 1: Cortical Thickness Discrimination (ADRC)

- Group analysis on ADRC (local) dataset
- The dataset consists of 42 AD and 50 Controls subjects
- Expect to find weaker signal but the same regions found from ADNI (small n)

Application 1: Cortical Thickness Discrimination (ADRC)

- Group analysis on ADRC (local) dataset
- The dataset consists of 42 AD and 50 Controls subjects
- Expect to find weaker signal but the same regions found from ADNI (small n)

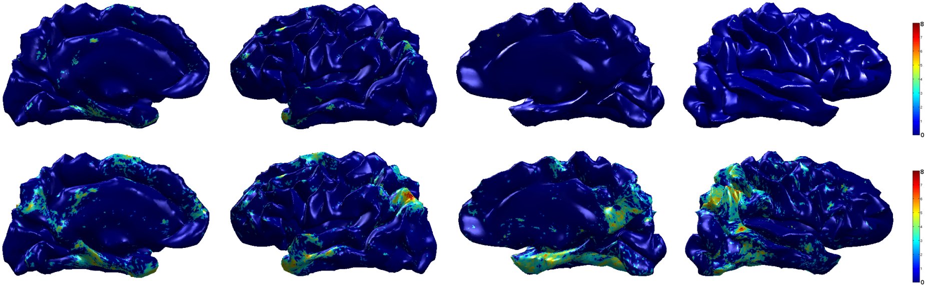

Figure: Group analysis on AD vs Controls. p-values in $-\log_{10}$ scale after FDR correction at $q = 0.05$ are shown on a smoothed brain surface. Top row: Result using smoothed cortical thickness, Bottom row: Result using WMD

Line Graph Transform

- We would like to detect group differences in brain connectivity.
- Here, the information lies on the edges of a graph, not on the vertices.
- We need to transform the graph G to apply our framework.

Line Graph Transform

- Line graph $L(G)$ is a dual form of graph G.
- Interchange of the roles of $\mathcal{V}$ and $\mathcal{E}$ in G.
- Let g_{ij} be the elements in the adjacency matrix $\mathbf{A_L}$ of $L(G)$,

$$g_{ij} = \begin{cases} 1 & \text{if} \quad v \in \mathcal{V}, \;\; v \backsim e_i, e_j \\ 0 & \text{otherwise} \end{cases}$$

where v is a vertex in $\mathcal{V}$ and e is an edge in $\mathcal{E}$.

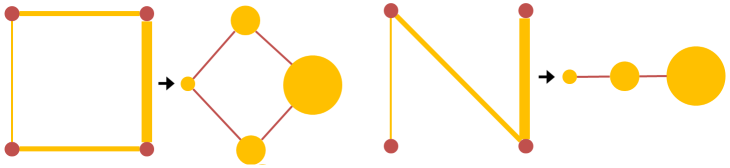

Figure: Examples of graphs and the corresponding line graphs. Original graphs with vertices (red) and edges (yellow) with edge weights (thickness), and corresponding line graphs with vertices (yellow) with function (vertex size) and edges (red).

Filtering Process on Line Graphs

- Once we obtain $L(G)$, we have a function defined on vertices.
- Now, we can apply filtering operations.
- Recall that wavelet transform is a band-pass filtering operation.
- An illustration of smoothing operation by line graph transformation.

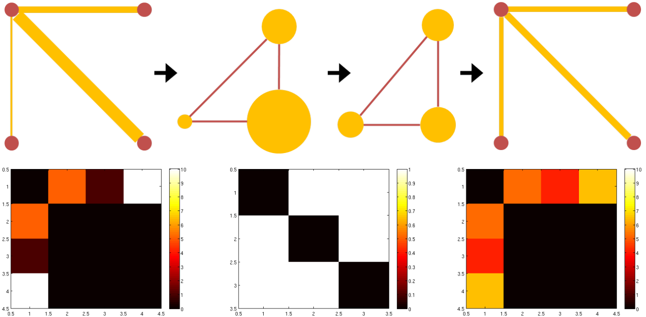

Figure: A toy example of graph structure filtering. The top panel shows the graph filtering steps: (1) Construction of the line graph, (2) filtering the signal on the line graph vertices, (3) reconstructing the filtered graph. The bottom panel shows the corresponding adjacency matrices.

Multi-scale Descriptor for Brain Connectivity

- Derive multi-scale descripter on $L(G)$ and transform back to G

Wavelet Connectivity Signature (WaCS)

$$\mathrm{WaCS}_f(e) = \{W_f(s, e) | s \in S\} \tag{2}$$

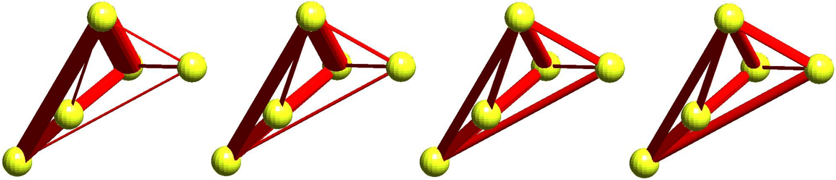

Figure: An example of multi-resolution on graph edges at various resolutions.

Application 2: Brain Connectivity Discrimination

ADRC and WRAP Dataset

- ADRC: 58 healthy vs. 44 AD subjects
- WRAP: 93 Family history (FH) positive vs. 250 negative subjects
- 162 parcellated brain regions as region of interest (ROI)
- Mean fractional anisotropy (FA) of tracts between ROIs
- 162×162 connectivity matrix for each subject

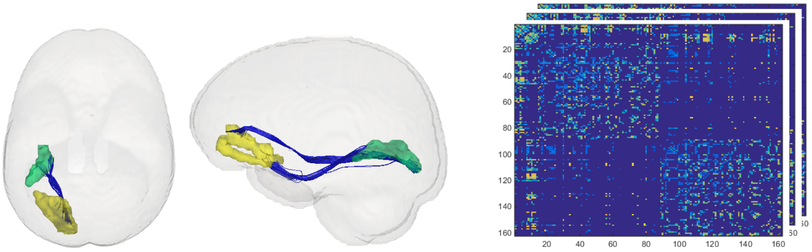

Figure: Left: ROIs and track bundles, Right: connectivity matrices.

Application 2: Brain Connectivity Discrimination

ADRC Study

Application 2: Brain Connectivity Discrimination

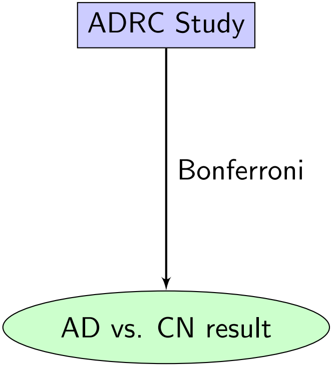

Application 2: Brain Connectivity Discrimination

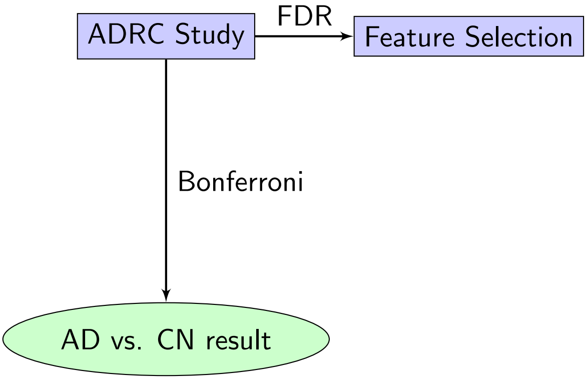

Application 2: Brain Connectivity Discrimination

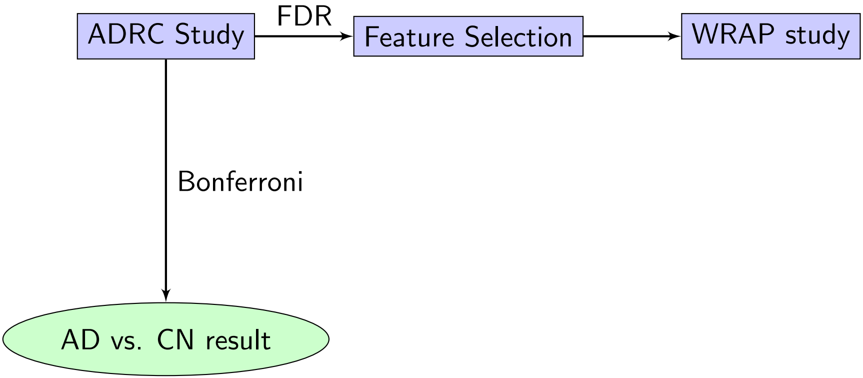

Application 2: Brain Connectivity Discrimination

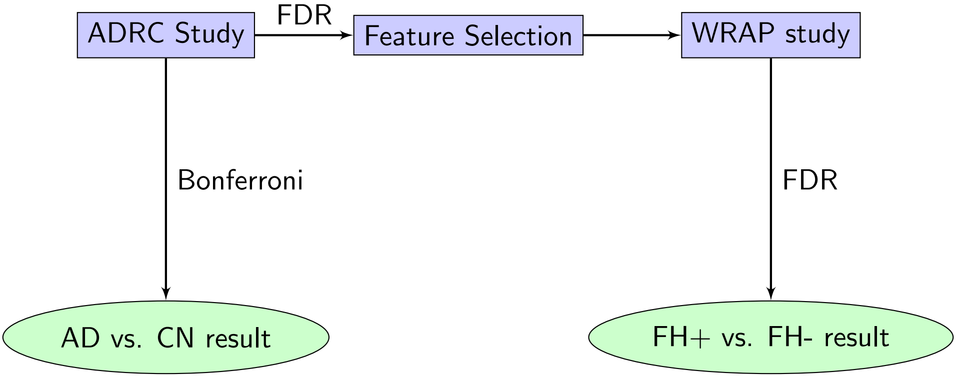

Application 2: Brain Connectome Discrimination - ADRC

- GLM on FA (control for age/gender) for p-values
- Bonferroni at $\alpha = 0.01$ for multiple comparisons correction
- The edge color represents the direction of difference
  - Red: stronger connection in Controls group
  - Blue: stronger connection in AD group

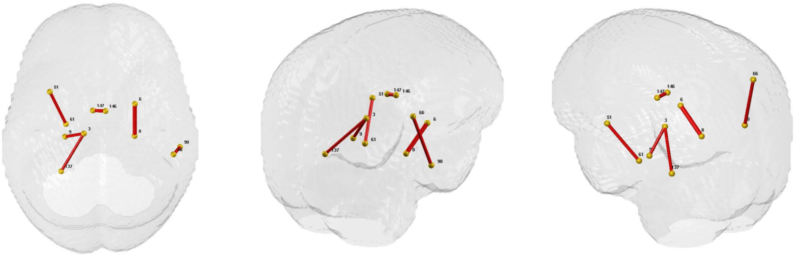

Figure: Significant connection difference between AD vs control group with direction of significance. Edge thickness corresponds to p-value, and the color denotes to the direction of strength.

Application 2: Brain Connectivity Discrimination - ADRC

- MGLM on WaCS (control for age/gender) for *p*-values
- Bonferroni at $\alpha = 0.01$ for multiple comparisons correction
- The edge color represents the direction of difference
  - Red: stronger connection in Controls group
  - Blue: stronger connection in AD group

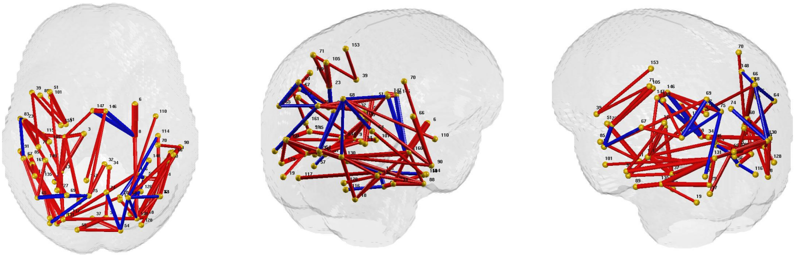

Figure: 81 significant connection difference between AD vs control group with direction of significance. Edge thickness corresponds to *p*-value, and the color denotes to the direction of strength.

Application 2: Brain Connectivity Discrimination - ADRC

- Hub regions: ROIs with connected edges ≥ 5
  - Left: superior and transverse occipital sulcus, superior parietal lobule,
  - Right: hippocampus, transverse occipital sulcus, precuneus, medial occipito-temporal gyrus

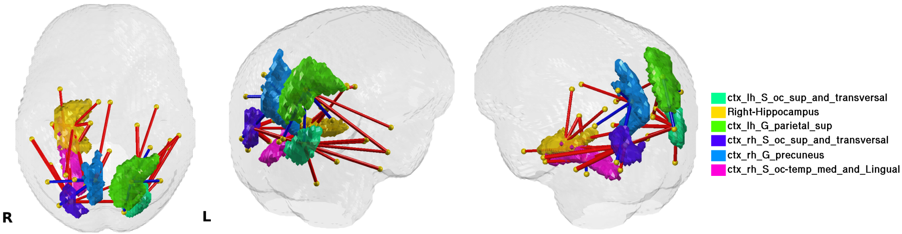

Figure: Illustration of the hub ROIs with connections identified as showing significant group difference between AD and control groups.

Application 2: Brain Connectivity Discrimination - WRAP

*Further Analysis on Preclinical AD (**small effect size**)*

- 615 Connections of interest (COIs) selected from ADRC study
- COI selection: FDR at 0.001 on AD vs. CN analysis
- Family History analysis on the COIs using WRAP data

Application 2: Brain Connectivity Discrimination - WRAP

*Further Analysis on Preclinical AD (**small effect size**)*

- Applying standard GLM analysis on FA revealed no connection
- MGLM (controlling for age/gender) for WaCS on COIs for *p*-values
- FDR at $\alpha = 0.05$ for multiple comparisons correction (less conservative than Bonferroni) to detect subtle variations

Application: Brain Connectivity Discrimination - WRAP

- 7 connections identified
  - Left: 5 ROIs (orbital gray matter, calcarine sulcus, lateral orbital sulcus, postro ventral cingular gyrus and pericallosal sulcus)
  - Right: 4 ROIs (precuneus, superior parietal lobule, posterior sylvian fissure, calcarine sulcus, pericallosal sulcus)

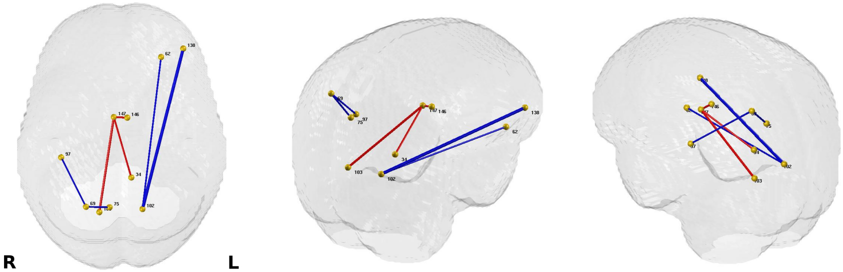

Figure: Significant group difference between FH+ and FH- groups. Color gives sign of strength: red (and blue) are stronger in FH- (and FH+ group).

Longitudinal Analysis of PIB Images

- W. H. Kim, B. B. Bendlin, M. K. Chung, S. C. Johnson, V. Singh, Statistical Inference Models for Image Datasets with Systematic Variations, CVPR, 2015.
- Longitudinal SUVR images from PIB scans from two time points

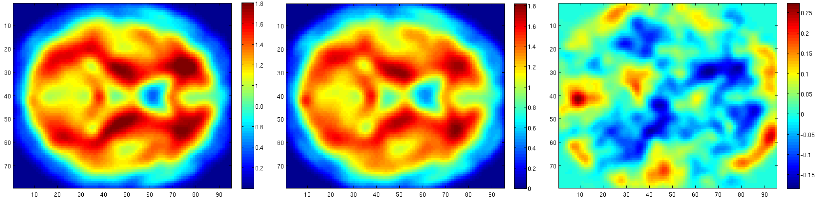

Figure: Changes of longitudinal SUVR images from a single subject. Decreases of the intensities are shown in various regions.

Analysis of Images with Imperfect Registration

- W. H. Kim, S. Ravi, S. C. Johnson, O. Okonkwo, V. Singh, On Statistical Analysis of Neuroimages with Imperfect Registration, ICCV, 2015
- Analysis with incorrectly registered brain images

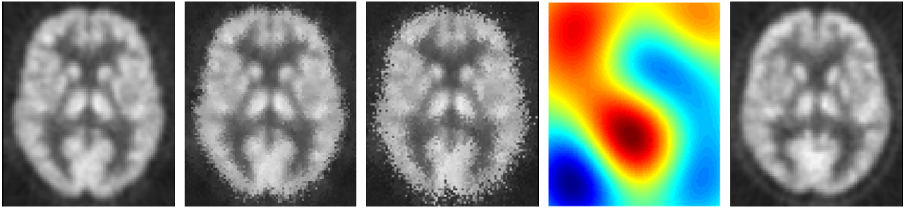

(a) (b) (c) (d) (e)

Figure: Registered FDG-PET scans of a subject. a) Using the original deformation field, b), c) Using deformation field with 5% and 10% noise level, d) A slice of GRF for spatially correlated noise, e) Using deformation field with d) as noise.

The BEMMA hammer (Dahl and Newton, 2006)

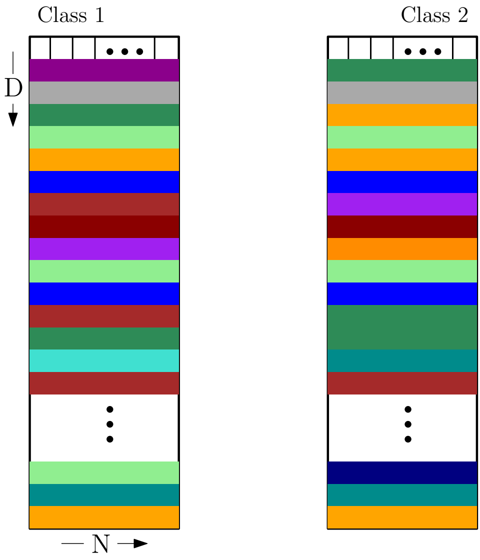

The BEMMA hammer (Dahl and Newton, 2006)

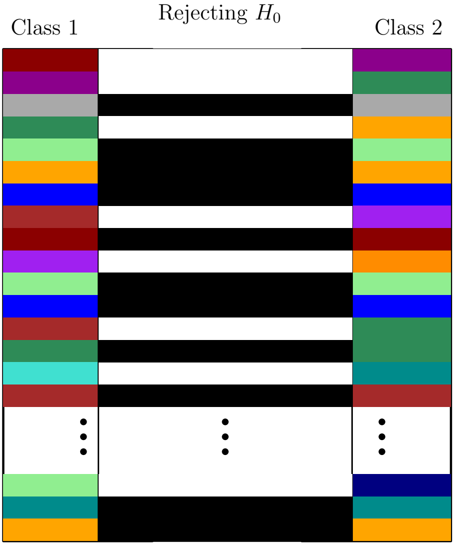

The BEMMA hammer (Dahl and Newton, 2006)

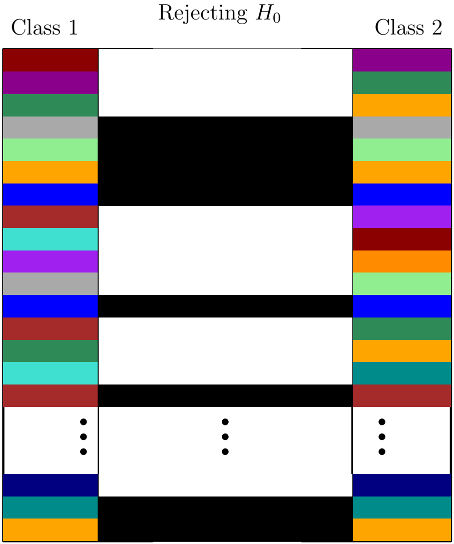

Graph restricted Chinese Restaurant Processes

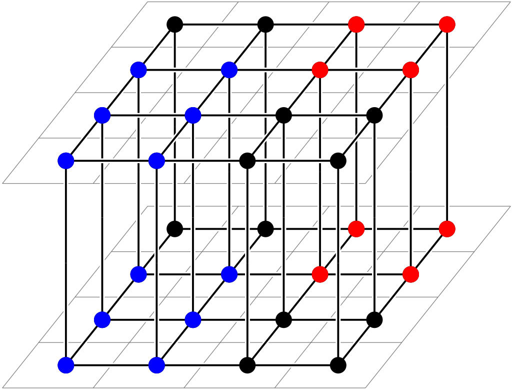

Graph restricted Chinese Restaurant Processes

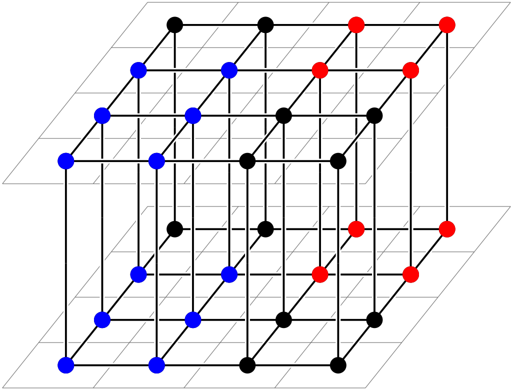

- The CRP is explicitly restricted by the image lattice
- Sampling must become significantly easier (relative to distance dependent CRPs)
- For cluster $\mathcal{C}_i$, improvements in statistical power $\propto |\mathcal{C}_i|$?

Conclusions

Conclusions

Thanks to the organizers!

Conclusions

- Powerful machinery for shape analysis of arbitrary meshes and graphs
- So far: has worked well on many different datasets and diverse application domains

Conclusions

- Powerful machinery for shape analysis of arbitrary meshes and graphs
- So far: has worked well on many different datasets and diverse application domains

  If you're interested –
- Start with the excellent papers by Maggioni and those by Hammond
- You may also look at some of our recent ones
  - Kim et al., NIPS 2012
  - Kim et al., NeuroImage 2014
  - Kim et al., NeuroImage 2015

Conclusions

- Powerful machinery for shape analysis of arbitrary meshes and graphs
- So far: has worked well on many different datasets and diverse application domains

  If you're interested –

- Start with the excellent papers by Maggioni and those by Hammond
- You may also look at some of our recent ones
  - Kim et al., NIPS 2012
  - Kim et al., NeuroImage 2014
  - Kim et al., NeuroImage 2015

Acknowledgments

Supported by NIH grants AG040396, AG021155, and NSF CAREER award 1252725. Also supported by UW ADRC AG033514, UW ICTR 1UL1RR025011 and UW CPCP AI117924.